Propagation of phase change front in monocrystalline SMA

Andre Chrysochoos, Christian Licht, Robert Peyroux

Propagation of Phase Change Front in Monocrystalline SMA

André Chrysochoos, Christian Licht, Robert Peyroux

Laboratoire de Mécanique et Génie Civil,
cc 048, Université Montpellier II,
34095 Montpellier Cedex 5, France

Abstract. Calorimetric effects related to the propagation of phase change front in a monocrystalline sample of CuZnAl shape memory alloy were derived from thermographic data analysis. During a load-controlled test, the displacement of the front induces a creep of the sample strongly depending on thermal exchanges with the surroundings. The main role played by the thermomechanical couplings can be pointed out by reversing the heat flux at the boundary of the sample: this leads to an inversion of the front propagation way associated with a recovery of the creep strain. We propose a behavioral modelling that takes into account the thermomechanical couplings accompanying the phase transition in single–crystal CuZnAl samples. The goal of this model is to put forward the significant role played by the heat diffusion in the propagation mode of the phase change fronts. Numerical simulations show the existence of phase change fronts such as the observed ones, and give good predictions of the calorimetric and kinematic effects accompanying the propagation.

1 Introduction

Strain induced by the propagation of phase change fronts during tensile tests on monocrystalline shape memory alloys (SMA) has already been evidenced in [1–3]. In this work, we propose to analyse the calorimetric effects linked to the propagation of these fronts using infrared image processing, and to employ a model, already presented in [4,5], to show that localization and propagation of phase change can be attributed without any ambiguity to coupling effects and heat diffusion. This model was already used to simulate the anisothermal behavior of polycrystalline sample of SMA, and allowed a correct prediction of the kinetics of phase change, the temperature variations and the associated strain (figures 1 and 2). The specificity of such o model is the way of taking into account the phase change mechanisms through strong thermomechanical couplings, the heat source related to phase change being the latent heat rate. Regarding the propagation of a phase change front, these notions are crucial, as they make it possible to determine the fields of strain, stress, temperature and volume fraction of phase change, and to track the propagation of the front.
In the following, we briefly recall the thermomechanical frame in which all the

work will be developed, present the experiments realized on monocrystalline sample, and propose a simple modelling of phase change front nucleation and propagation.

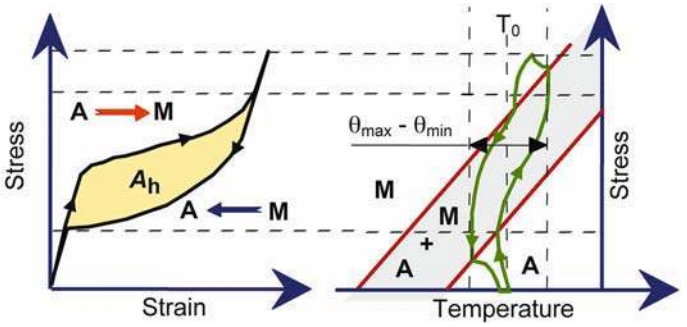

Fig. 1. Pseudoelastic behaviour and width of the transition domain

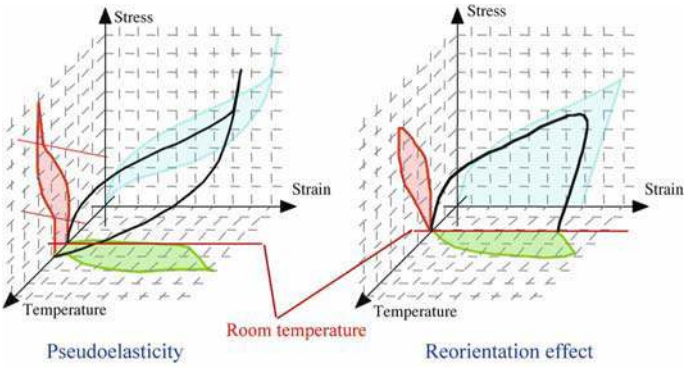

Fig. 2. Pseudoelastic and reorientation effects in a stess-strain-temperature space

2 A convenient thermomechanical framework

A convenient thermodynamic framework is the Continuum Thermodynamics [9], that postulates the local state axiom and considers the material both as a continuum and as a thermodynamic system described by a set of state variables. More precisely, we use the formalism of Generalised Standard Materials (GSM) [10] for which the constitutive equations can be derived from a

thermodynamic potential and a dissipation potential. The chosen set of variables is $\{T, \varepsilon, x\}$, T being the temperature, ε the strain tensor and x referring to the volume fractions of martensite.
Using the formalism of GSM, a thermodynamic potential $\psi(T, \varepsilon, x)$ (specific Helmholtz free energy) and a dissipation potential $\varphi(gradT, \dot{\varepsilon}, \dot{x})$ are introduced. Their derivatives with respect to the state variables and their time derivatives give the state equations (1a) and the evolution equations (1b).

$$a) \begin{cases} s = -\Psi_{,T} \\ \sigma^r = \varrho\Psi_{,\varepsilon} \\ A = \varrho\Psi_{,x} \end{cases} \qquad b) \begin{cases} q = \varphi_{,grad\ T} \\ \sigma^{ir} = \varphi_{,\dot{\varepsilon}} \\ A = -\varphi_{,\dot{x}} \end{cases} \qquad with\ \sigma = \sigma^r + \sigma^{ir} \tag{1}$$

where σ, q, s, ϱ and A stand for the stress tensor, the heat influx vector, the specific entropy, the mass density and the thermodynamic force associated with x, respectively. Note that A is defined such as the product $-A\dot{x}$ is the part of dissipated energy corresponding to the phase transformation.
The local heat conduction equation can be derived from the two principles of thermodynamics in the following form,

$$\varrho C\dot{T} - k\Delta T = d_1 + \varrho T\psi_{,T\varepsilon} : \dot{\varepsilon} + \varrho T\psi_{,Tx} .\dot{x} = w_h \tag{2}$$

where C denotes the specific heat capacity, and k the coefficient of thermal conduction. The quantity d_1 represents the intrinsic dissipation and w_h stands for the volume heat source generated by all the terms in the right hand of equation 2. This last term can be experimentally evaluated using temperature fields given by an infrared camera (see [6] for more details).

3 Experimental analysis.

3.1 Material data

Quasi-static tension tests were performed at constant room temperature on a cylindric sample (diameter 3.85mm, length 24mm). The material is a monocrystalline shape memory alloy of type $Cu_{70}Zn_{25}Al_4$. The main thermomechanical data of this alloy are gathered in the following table. The room temperature is chosen such as the sample is austenitic at the beginning of the test.

specific mass	specific heat capacity	thermal conduction	expansion coefficient	latent heat
ϱ (kg.m^{-3})	C (J.kg^{-1}.K^{-1})	k (W.m^{-1}.K^{-1})	α (K^{-1})	C (J.kg^{-1}.K)
7800	390	120	1.9 10^{-7}	7000

elastic modulus	transformation strain	expansion coefficient	austenite temperatures	martensite temperatures
E (GPa)	β	α (K^{-1})	As °C Af	Ms °C Mf
7800	8. 10^{-2}	19. 10^{-5}	22 29	23 12

3.2 Experiments

The mechanical loading imposed during this test consists of three stages (see figure 3a):
- stage a–b: force loading of the sample ($\dot{F} = 93$ N.s^{-1}).
- stage b–c: force hold at 885 N during 2 minutes.
- stage c–d: return to zero force ($\dot{F} = -93$ N.s^{-1}).

The evolution of a temperature profile along one generating line of the sample is presented versus time in figure 3b. In the same way, the corresponding heat sources are plotted in figure 3c.
The very first part of the loading (a–a') is associated with the elastic behavior of the material, involving small temperature variations and slight deformation of the sample. At time a', strong and positive heat sources concentrate at the bottom of the sample, in a zone moving during the loading (a'–b). The displacement of this zone is linked to the propagation of a phase change front (austenite/martensite exothermal transformation). When the stress is held constant (b–c), sources of lower intensity are observed, and the zone where they concentrate moves slower. The associated phase transformation involves also a localized strain and consequently a displacement of the cross–head (also plotted in figure 3a). This displacement is comparable to the one observed in creep when dealing with viscoelastic materials, but here the time–dependency is not linked to viscosity but to heat diffusion. Finally, we observe during the unloading stage (c–d) the propagation of a zone where negative heat sources are concentrated (martensite/austenite endothermal transformation).
For all the different stages, and due to heat diffusion, phase change localization is easier to track from heat sources analysis than from temperature fields. Indeed, the evolution in time of temperature in one characteristic point results from all heat transfer modes: conduction of the latent heat within the sample and convection, radiation and conduction of heat between the sample and the surroundings. Nevertheless, analysis of heterogeneous temperature profiles is consistent with the existence of wave–like front moving along the sample, the maximum amplitude of temperature variations being roughly associated with the current position of the front.

The propagation of the phase change front is tightly related to thermomechanical couplings. Calorimetric effects associated to phase change result in temperature variations, these variations playing a part in the phase change kinetics. Remind that the amplitude of temperature evolution during the test (around 5°C) is of the same order of magnitude that the width of the transition domain (around 11°C) (Fig. 1). The local mechanical response is consequently depending on temperature, the temperature resulting from the rate of latent heat and from the thermal exchange in the sample and with the surroundings. During stage b–c, when the force is kept constant, the front propagation speed is directly linked to the heat exchanges with the exterior. The creep–like displacement is governed by thermal diffusion. As a matter of

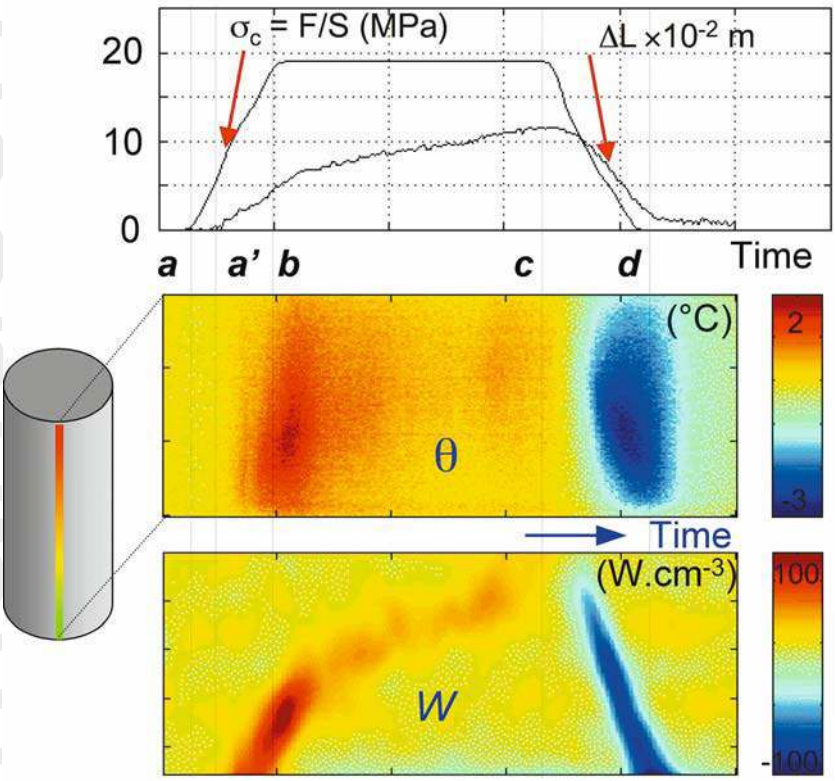

Fig. 3. Time evolutions of stress and cross-head displacement (a), of temperature variations θ (b), and of heat sources W_h (c) along the sample

proof, we increased the convection exchange coefficients using a fan, and we observed higher front propagation speeds (figure 4a and b). One can obtain up to an inversion of phase change way (figure 4c) by reversing the exchanged heat flux (this is done by a rapid increase of the surrounding temperature above the sample maximum temperature).

4 Modelling and numerical simulations

In this part, a one-dimensional version of the model developed in [4] is presented. The aim of this modeling is to show that localization and propagation of phase change, as experimentally observed, may be attributed without ambiguity to coupling effects and to heat diffusion.

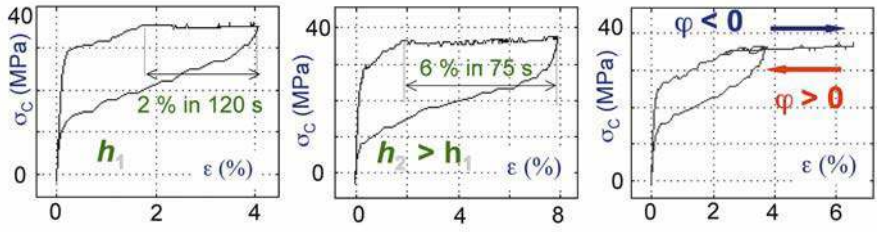

Fig. 4. Mechanical responses of the sample for two different values of the heat exchange coefficient, and creep and "reverse creep" due to heat flux ϕ inversion

4.1 A one-dimensional thermomechanical model

Indeed, this model considers the phase change as a strong coupling mechanism, the dissipation of which remains weak in comparison with the latent heat rate [7]. The state variables associated to the model are the temperature variations θ with respect to the equilibrium temperature T_0, the longitudinal strain ε and the volume proportion of martensite X. The specific energy ψ and the dissipation potential ϕ are chosen as follows:

$$\psi(\theta,\varepsilon,X) = \frac{E}{2\varrho}(\varepsilon - \alpha\theta - X\beta)^2 - \left(\frac{C}{2T_0} + \frac{E\alpha^2}{2\varrho}\right)\theta^2 + \frac{K\beta}{\varrho}\left(\frac{A-M}{2}X^2 + (T-A)X\right) + I_{[0,1]}(X) \tag{3}$$

$$\varphi\left(\frac{\partial\varepsilon}{\partial t}, \frac{\partial X}{\partial t}, \frac{\partial\theta}{\partial x}; T\right) = \frac{k}{2T}\left(\frac{\partial\theta}{\partial x}\right)^2 \tag{4}$$

where K, A and M are three characteristic constants defining the transition domain in the plane (θ,σ) (Fig. 5). According to this choice of ψ and φ, the strain can be split into an elastic, a thermal and a transformation part ($\varepsilon = \sigma/E + \alpha\beta + X\beta$), and the kinetics of phase change is found to be a linear evolution of X between the borders of the domain (Fig. 5). The heat equation (5) neglects the convective terms of the particular time derivative, takes account of lateral heat losses (characteristic time τ) and considers the two coupling heat sources induced by thermal dilatation and phase change. Finally, heat exchanges at the ends of the sample are characterised by Fourier conditions (Fig. 5).

$$\varrho C\left(\frac{\partial\theta}{\partial t} + \frac{\theta}{\tau}\right) - k\frac{\partial^2\theta}{\partial x^2} = -E\alpha T_0\frac{\partial\varepsilon}{\partial t} + \varrho L_0\frac{\partial X}{\partial t} \tag{5}$$

Note that the latent heat L_0 can be written $L_0 = (E\alpha + K)\beta T_0/\varrho$.

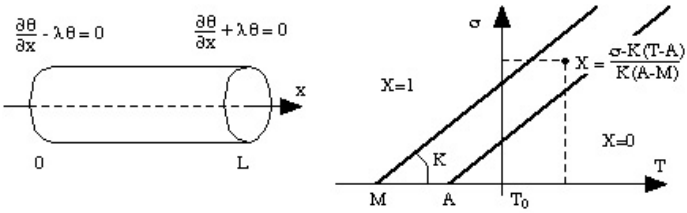

Fig. 5. Gauge part of the sample with thermal boundary conditions and transition domain

4.2 Numerical results

The numerical simulations were performed using a sample of 24 mm length and 3.855 mm diameter. The value of the longitudinal heat exchange coefficient λ is 1872 $W.m^2.K^{-1}$, and the characteristic time τ is 586 s. Owing to the symmetry of the problem, only half a sample is considered.
On the one hand, diffusion effects, amplified by couplings mechanisms, yield to uniform temperature fields. On the other hand, stress remains uniform within the sample during uniaxial quasi-static loading. One can thus expect that phase transition occurs within as narrow as the width $A - M$ of the transition domain is small. The limit case corresponds with a unique transition line, traditionally introduced in thermodynamics of phase transition with change of state [8]. Consequently, a value of 0.01 °C has been chosen for $A - M$. The numerical results in term of temperature and heat sources evolutions are found to be consistent with the experimental ones (Fig. 6), and the "creep" and "anti-creep" phenomena are qualitatively satisfying. Computations also show a hysteresis loop in good agreement with experimental observations even though the model supposes that the intrinsic dissipation equals to zero. In this case, hysteresis arises from two conjugate effects: thermomechanical couplings (material effect) and heat diffusion (material and structure effect).

4.3 On transition temperatures

To characterize a SMA monocrystal, the present model uses only two transition temperatures named A and M. The choice of a very small value for the difference $A-M$, corresponding to the width of the transition domain, is not incompatible with the classical way of defining the four transitions temperature A_s, A_f, M_s, M_f. Figure 7 presents a virtual dilatometry test where these four temperatures correspond to slope changes in the stress–strain response. The difference between M_s et M_f can reach 10°C for a transition domain of the monocrystal of 0.01 °C. The hysteresis area is then induced by the heat losses during the phase transition. Consequently, the four above-mentioned temperatures are depending on the sample geometry and on the heat exchange conditions. They are no longer intrinsic parameters of the material.

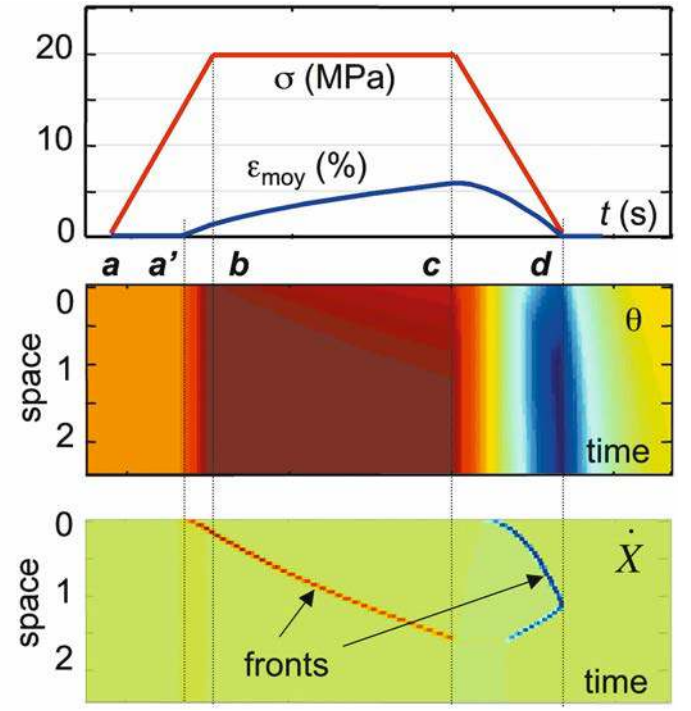

Fig. 6. Mechanical loading and sample stretching, temperature field θ, and latent heat rate pattern $\dot{X}$

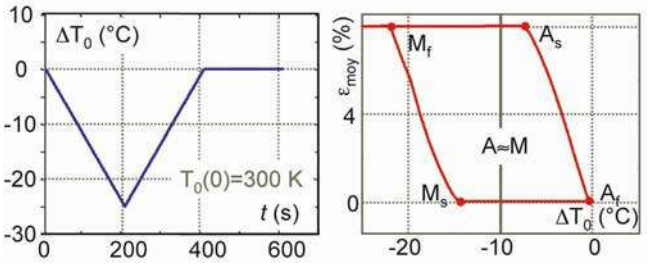

Fig. 7. Virtual dilatometry test showing the four transitions temperatures of the sample

5 Discussion

The main purpose of this paper is to point out the importance of the thermomechanical couplings on the material behavior. In particular, it underlines the dependance of the mechanical response on the temperature and the structure effects induced by the heat diffusion in the volume of the sample. The amazing mechanical effects observed and modelled in this work (for instance "creep" and "anti-creep" phenomema) are the consequences of the time–dependency through heat diffusion. When the phase change is localized in a front, the heterogeneous distribution of heat sources increases the influence of heat losses and amplifies the interaction between material and structure.

References

1. Shaw J.A., Kyriakides S., Thermomechanical aspects of NiTi, J. Mech. Phys. Solids 43 (1995) 1243-81.
2. Orgeas L., Favier D., Stress-induced martensitic transformation of a NiTi alloy in isothermal shear, tension and compression, Acta mater. 46 (1998) 5579-91.
3. Liu Yi., Liu Yo., Van Humbeeck J., Luders-like deformation associated with martensite reorientation in NiTi, Scripta Materialia 39 (1998) 1047-55.
4. Peyroux, R., Chrysochoos, A., Licht, C., Löbel, M., 1998; Thermomechanical couplings and pseudoelasticity of shape memory alloys, Int. J. of Engng. Sci., Vol. 36, n° 4, pp. 489-509.
5. Balandraud X., Chrysochoos A., Leclercq S., Peyroux R., Effet du couplage thermomcanique sur la propagation dun front de changement de phase, C.R. Acad. Sci. Paris, t.329, Srie II b, (2001), 621-626.
6. Chrysochoos, A., 1995; Analyse du comportement thermomé canique des matériaux par thermographie infrarouge, Photomécanique 95, Ed. Eyrolles, pp.203-211.
7. Chrysochoos, A., Löbel, M., 1996; A thermomechanical approach to martensite phase transition during pseudoelastic transformation of SMAs, in K.Z. Markov (Ed.), Proc. of the 8th Int. Symp. n Continuum Models and Discrete Systems, World Scientific, pp. 21-29.
8. Callen, H.B., 1985; Thermodynamics and an Introduction to Thermostatics, Wiley, pp. 215-253.
9. Germain, P., 1973; Cours de Mécanique des Milieux Continus, Masson et Cie Ed., p. 417
10. Germain,P., Nguyen Q.S., Suquet, P., 1983; Continuum Thermodynamics, J. of Appl. Mech., Transactions of the ASME, 50, pp. 1010-1020.
11. Halphen, B., Nguyen Q.S., 1975; Sur les Matériaux Standards Généralisés, Journal de Mécanique, Vol. 14, pp 39-63.